A Theoretical Study of One- and Two-Photon Activity of D-Luciferin

Mausumi Chattopadhyaya [1],*,† and Md. Mehboob Alam [1,2],*,‡

[1] Department of Chemistry, University of Calcutta, 92 A.P.C. Road, Kolkata 700009, India
[2] Laboratoire de Chimie Quantique, Institut de Chimie, CNRS/Université de Strasbourg, 4 rue Blaise Pascal, Strasbourg 67000, France
* Correspondence: mau.chem@yahoo.co.in (M.C.); mehboob.cu@gmail.com (M.M.A.);
     Tel.: +49-308-413-4814 (M.C.)
† Current address: Fritz-Haber-Institut der Max-Planck-Gesellschaft, Faradayweg 4-6, 14195 Berlin, Germany.
‡ Current address: Department of Chemistry, Universitetet i Tromsø–Norges Arktiske Universitet,
     Hansine Hansens veg 18, 9019 Tromsø, Norway.

Abstract: In the present work, we have theoretically studied the one and two-photon absorption (OPA and TPA) probabilities of the native D-luciferin molecule and attempted to find the origin of its larger TPA cross-sections in polar solvents than in non-polar ones. The calculations using state-of-the-art linear and quadratic response theory in the framework of time-dependent density functional theory using hybrid B3LYP functional and cc-pVDZ basis set suggests that two-photon transition probability of this molecule increases with increasing solvent polarity. In order to explicate our present findings, we employed the generalized few-state-model and inspected the role of different optical channels related to the TPA process. We have found that the two-photon transition probability is always guided by a destructive interference term, the magnitude of which decreases with increasing solvent polarity. Furthermore, we have evaluated OPA parameters of D-luciferin and noticed that the the excitation energy is in very good agreement with the available experimental results.

Keywords: two-photon absorption; solvent effect; channel interference; computational chemistry; non-linear optics; few-state model; response theory; TD-DFT

1. Introduction

Two-photon absorption (TPA) process (i.e., the simultaneous absorption of two photons stimulated by an intense laser beam) is related to the imaginary part of the third order non-linear optical susceptibility. Unlike the absorption/emission of a single photon, it is dependent on the square of the intensity of the incident light [1], which gives rise to a large spatial confinement. This means that the non-linear effect produced by the TPA process mainly occurs at the focal volume, which in turn makes this process better for fluorescence imaging [2]. The resolution increases, and better quality images are obtained compared to those obtained from conventional confocal imaging. Apart from this, TPA process is also excellent for in vivo imaging, because of its larger penetration depth and lower phototoxicity. The latter is because of the use of infrared photons, which are safe for live cells, and hence do not cause cell damage. Because of its larger penetration depth, the TPA process is also very useful for the treatment of thick specimen samples. Additionally, the different selection rules obeyed by the TPA process makes it efficient for accessing those excited states which are otherwise inaccessible. These features make the TP active materials highly demanding for many applications, including optical power limiting [3], photodynamic therapy [4,5], lithography [6], micro fabrication [7],

and three-dimensional (3D) optical data storage [8]. The unprecedented surge of research interest in this area has been focused on finding out the proper design principle, followed by the synthesis of molecules with large TPA cross-section. This is guided by a number of factors, such as conjugation length [9,10], donor/acceptor (D/A) strength [11,12], molecular symmetry [13], through space charge transfer interaction [14], branching of diploes and quadrupoles [15], formation of excitons and the open-shell character of the biradical systems [16]. The potential application of D/A substituted trans-stilbene in optical power limiting was pointed out by Albota et al. [3]. Prasad et al. [17] have reported many chromophores as TP active materials. Ruud and Chakrabarti have designed a new class of compounds, known as tweezer-TNF and reported the long-range through space charge-transfer (TSCT) interaction in TP absorption [14]. They also studied the role of weak-interaction in controlling the TPA intensity in the IR-wavelength region. Chattopadhyaya et al. [18] have shown that the number of D/A groups cannot be the sole criteria for larger TPA cross-section; rather, the D/A groups at a suitable position can lead to a large dipole moment difference between the ground and excited state, which is ultimately responsible for the high TP activity of bisanthene and D/A substituted bisanthene molecule. Apart from all these factors, Cronstrand et al. [19,20] and Alam et al. [21,22] have shown that as the excitation from ground to excited state takes place through several optical pathways by the involvement of several intermediate states, the interference between different optical channels also have a crucial role in determining the overall TP activity of a molecule. Cronstrand et al. have scrutinized the role of interference between different optical channels and derived a two-dimensional four-state model formula to demonstrate the role of some selective chromophores on TP activity. Alam et al. [21] have derived a generalized-few-state model (GFSM) including the channel interfering terms for 3D molecules. The interfering terms depending upon the alignment of the transition dipoles may either be constructive or destructive, and have a direct impact on TP transition probability of a molecule. Moreover, several ab initio investigations have been performed to study the crucial role of solvents in determining the TP transition probability [23–25]. Alam et al. [26–28] have made a thorough investigation on the role of solvents as well as the interfering terms, and argued that the constructive interference between the different optical channels increases in moderately polar solvent. In an another work, they reported on some TSCT systems where the TP transition probability decreases with increasing solvent polarity [26]. They also showed that the destructive interference increases with increasing solvent polarity.

In the present work, we have selected the native D-luciferin molecule and calculated the gas and solvent phase one- and two-photon absorption parameters using linear and quadratic response theory. We have found that TP transition probability of native D-luciferin increases with increasing solvent polarity. To find the precise origin of this, we have made an in-depth analysis of the interference between the several optical channels by means of GFSM for 3D molecules, and confirmed that the magnitude of destructive interference decreases with increasing the solvent polarity.

2. Computational Details

The ground state geometry of the native D-luciferin molecule has been optimized both in gas phase, C_2H_5OH, $C_6H_5CH_3$, and C_6H_{12} solvents using hybrid B3LYP functional and Pople's 6-31G(d,p) basis set for C, H, N, O, and an effective core potential (ECP)-corrected LANL2DZ basis set for S atoms. In the following work, ECP has been used to save some computational time. The TP cross-section obtained with or without ECP is expected to have the same order of magnitude, because TPA does not involve the inner electrons, and hence a suitable pseudopotential (which is the case for S-atom) should not affect the process—and hence the computational results—drastically. The solvent phase geometry optimizations have been carried out within a polarizable continuum model (PCM) [29,30], as implemented in Gaussian 09 program package [31]. In the next step, we have performed frequency calculations on each optimized geometry using the same level of theory as used for the geometry optimization. The absence of any imaginary frequency proved the true variational minima of the ground state electronic wave function. The geometry optimization and the frequency calculations have

been done in the Gaussian 09 suite of programs. On these optimized geometries of native D-luciferin (Figure 1), we have performed linear and quadratic response theory calculations for evaluating one- and two-photon absorption parameters using Dunning's cc-pVDZ basis set and B3LYP functional. The response calculations have been performed within non-equilibrium PCM [32,33], as implemented in the DALTON code [34,35]. The PCM-based response calculation in DALTON uses a spherical cavity model in which the solvent cavities are considered as an interlocking sphere. We have considered the cavity radii of 2.28 Å, 2.04 Å, 1.8 Å, and 2.108 Å for C, N, O, and S atoms, respectively. These radii are found to cover the whole molecule in a single solvent envelope. The static and optical dielectric constants of different solvents considered in this work are the default values implemented in the DALTON code. We have reevaluated the two-photon transition probability of D-luciferin using a GFSM model where we have made an in-depth analysis of the different angles between the transition dipole moment vectors and different interfering terms.
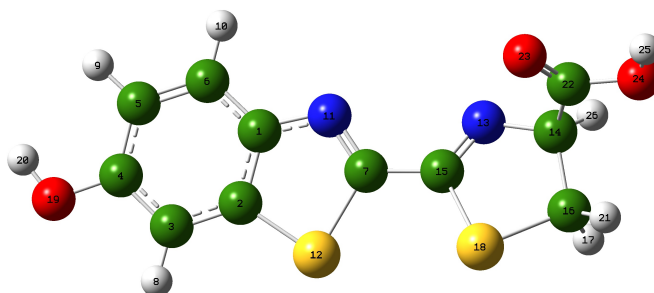

Figure 1. Gas phase optimized geometry of native D-luciferin molecule. Green, white, yellow, blue, and red colors represent C, H, S, N, and O atoms respectively.

3. Results

3.1. Geometry of the Studied System

The gas phase optimized geometry of native D-luciferin is presented in Figure 1. The gas and solvent phase optimized D-luciferin molecule belongs to C_1 point group. It is clearly manifested from the optimized geometry that the main skeleton of the native D-luciferin molecule is near to planar configuration, though the particular ring bearing the chiral centre is making a small dihedral with the indene-type fused moiety. The important geometric parameters are presented in Table 1 and Table 2. The dihedral angle between the indene-type fused ring and ring-bearing chiral centre is presented in Table 1. Three different types of dihedral angles are considered here to describe the geometry of D-luciferin. A close inspection of Table 1 reveals that these dihedral angles are not changed significantly on changing the media from gas phase to solvent phase. Different bond lengths, including three different types of C-O and two different types of C-S, C-N, and C-C bonds lengths are presented in Table 2. The data in Table 2 shows that these bond lengths—like the dihedral angles in Table 1—remain unchanged on moving from gas phase to solvent phase.

Table 1. Different dihedral angles (in degree) of native D-luciferin molecule, both in gas and solvent phase.

Dihedral Angle	Gas	C_6H_{12}	C_2H_5OH	$C_6H_5CH_3$
S_{12}-C_7-C_{15}-N_{13}	158.34	158.67	158.33	158.70
S_{12}-C_7-C_{15}-S_{18}	−21.83	−21.54	−22.28	−21.52
N_{11}-C_7-C_{15}-N_{13}	−21.31	−20.95	−21.48	−20.92

Table 2. Different bond lengths (Å) of native D-luciferin molecule both in gas and solvent phase.

Bond Length	Gas	C_6H_{12}	C_2H_5OH	$C_6H_5CH_3$
C_{22}-O_{24}	1.359	1.354	1.346	1.353
C_{22}-O_{23}	1.198	1.200	1.205	1.201
C_4-O_{19}	1.366	1.365	1.363	1.365
C_7-S_{12}	1.834	1.835	1.829	1.834
C_{15}-S_{18}	1.851	1.848	1.842	1.848
C_7-N_{11}	1.284	1.285	1.288	1.285
C_{15}-N_{13}	1.265	1.266	1.269	1.267
C_7-C_{15}	1.467	1.467	1.467	1.467
C_{14}-C_{22}	1.534	1.534	1.54	1.534

3.2. One-Photon Absorption

We started our investigation by evaluating the one-photon absorption (OPA) parameters for the first two singlet transitions; namely, S_0-S_1 and S_0-S_2 states of the native D-luciferin molecule using the gas and solvent (cyclohexane, ethanol, and toluene) phase optimized geometries using cc-pVDZ basis set and B3LYP functional. Irrespective of the nature of solvent, the values of excitation energies for the two transitions are very close to each other, with a maximum difference of 0.19 eV (in toluene). However, the values of oscillator strengths for the two transitions differ largely and show a maximum difference of 0.4 a.u. (in solvent phases). To study the effect of range-separated functional on the OPA parameters, we have re-evaluated the said parameters using long range corrected CAM-B3LYP functional and cc-pVDZ basis set. In an earlier experimental study [36], the OPA wavelength for native D-luciferin molecule was reported as 319 nm, and our calculations using CAM-B3LYP and B3LYP functional with cc-pVDZ basis set (in gas phase) have yielded a value of 284.39 and 321.38 nm, respectively, corresponding to the S_0-S_1 transition. As the OPA wavelength obtained using B3LYP functional matches well with the experimental value and is underestimated by the CAM-B3LYP functional, we have carried out the rest of the calculations with B3LYP/cc-pVDZ level of theory. The excitation energy, oscillator strength, transition moment, and other important OPA parameters computed for native D-luciferin molecule both in gas and solvent phase has been tabulated in Table 3.

Table 3. Excitation energy, oscillator strength, transition moment, lambda value, and the contributing orbitals for the first two transitions of D-luciferin in gas, ethanol, toluene, and cyclohexane solvents.

Excited State	Solvent	Excitation Energy (eV)	Oscillator Strength (a.u.)	Transition Moment				Λ	Orbital Contributions
				X	Y	Z	Total		
1	Gas	3.85	0.247	−1.618	−0.209	−0.119	1.636	0.674	H-L
	C_2H_5OH	3.73	0.439	−2.191	−0.434	−0.102	2.236	0.686	H-L
	$C_6H_5CH_3$	3.77	0.447	−2.200	−0.414	−0.110	2.241	0.698	H-L
	C_6H_{12}	3.78	0.431	2.157	0.398	0.110	2.916	0.699	H-L
2	Gas	3.93	0.112	1.072	0.479	−0.057	1.175	0.530	H-1-L
	C_2H_5OH	3.92	0.017	0.345	0.366	−0.117	0.517	0.501	H-1-L
	$C_6H_5CH_3$	3.91	0.030	−0.518	−0.413	0.106	0.672	0.501	H-1-L
	C_6H_{12}	3.91	0.031	−0.566	−0.420	0.102	0.712	0.501	H-1-L

A close inspection of the results in Table 3 reveal that the excitation energy for the S_0-S_1 transition in gas phase is larger in magnitude than that in solvent phase. Furthermore, the excitation energy for the first excited state increases with decreasing polarity of the solvent. For the second transition (namely, S_0-S_2), the value of excitation energy is highest in gas phase, and it reflects an insignificant impact of the solvent polarity. These results indicate that the first excited state in D-luciferin is more polar than its second excited state. We also noticed that the first excited state in gas phase is much less one-photon active than it is in solvent phases. The oscillator strength in toluene, cyclohexane, and ethanol solvents are comparable with each other. In contrast to this, for the second excited state, the oscillator strength in gas phase is much larger than that in solvent phases. Irrespective of the nature of the solvent, the first excited state is always more one-photon active than the second excited state.

This different one-photon activities can be well explained by considering the effect of excitation energy and transition dipole moment vectors on oscillator strength. Theoretically, the oscillator strength for the $|0\rangle \rightarrow |f\rangle$ transition is given by

$$\delta_{\text{OPA}} = \frac{2\omega_f |\mu^{0f}|^2}{3},$$

(1)

where $\mu^{0f} = \sqrt{\sum_\alpha |\langle 0|\hat{\mu}_\alpha|f\rangle|^2}$, $\hat{\mu}_\alpha$ is the αth component of transition dipole moment operator, and ω_f is the excitation energy for the $|0\rangle \rightarrow |f\rangle$ transition. Here, $\alpha \in x, y, z$. It is obvious from Table 3 that in spite of having larger ω_f for the first excited state in gas phase, the corresponding transition dipole moment value is much less than that in solvent phases. That is why δ_{OPA} for the first excited state is much less than that in solvent phases. For the second excited state, μ^{0f} is much less than the first excited state, which explains the larger one-photon activity of the latter. We have also noticed that the x-component of μ^{01} is the most contributing component, whereas for μ^{02}, both the x and y components are contributing almost equally. This indicates that the first transition is mainly dominated by the charge-transfer from the donor to the acceptor group, whereas the second one has more contribution from the re-organization of the π electrons throughout the molecule.
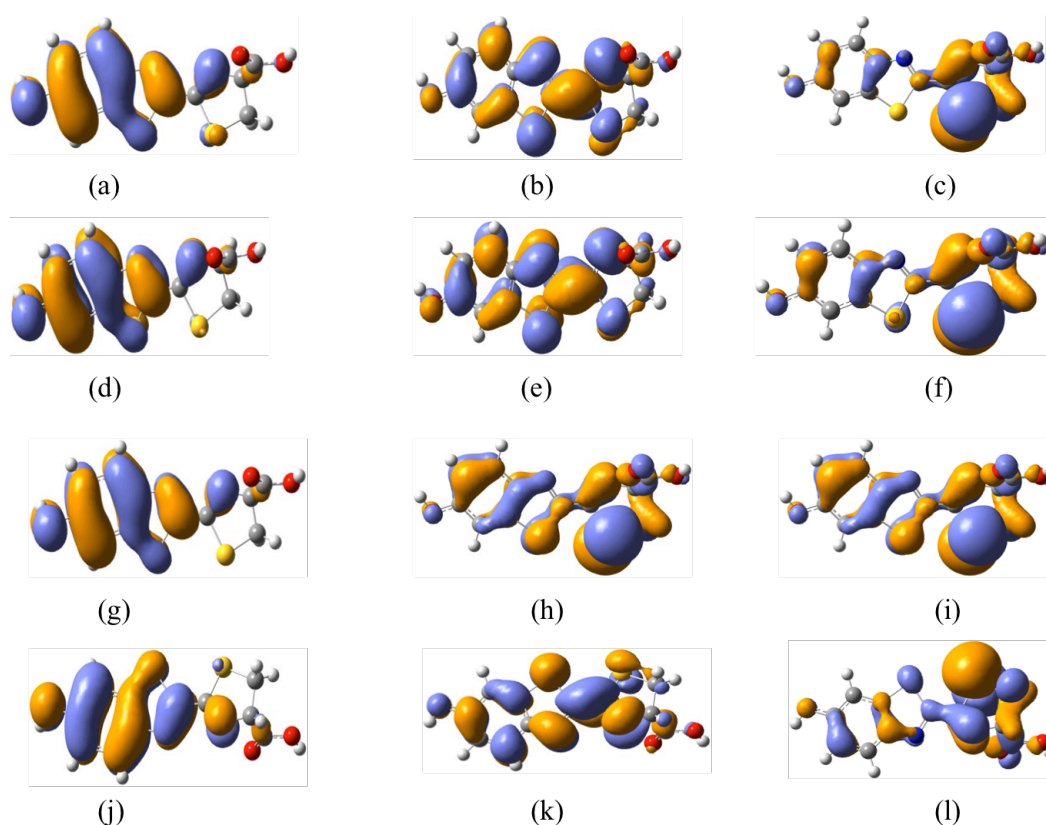

(a)　　　　　　　　　　(b)　　　　　　　　　　(c)

(d)　　　　　　　　　　(e)　　　　　　　　　　(f)

(g)　　　　　　　　　　(h)　　　　　　　　　　(i)

(j)　　　　　　　　　　(k)　　　　　　　　　　(l)

Figure 2. HOMO, LUMO, and HOMO-1 of D-luciferin molecule: (**a**–**c**) in gas phase; (**d**–**f**) in cyclohexane; (**g**–**i**) in ethanol; and (**j**–**l**) in toluene solvent.

In order to study the directionality and short-/long-range nature of the two transitions, we have calculated the Λ parameter and the corresponding orbital contributions. The Λ parameter—whose value always lies between 0 and 1—is calculated from the inner product between the moduli of each pair of occupied and virtual orbitals involved in a transition. Therefore, a larger values of Λ indicates a short-range nature of the transition, whereas a smaller value indicates a long-range transition.

The results for Λ parameter and orbital contributions are also shown in Table 3. The orbital contributions clearly indicate that for the S_0–S_1 transition, the only significant contribution comes from HOMO–LUMO orbital transition. Similarly, the S_0–S_2 transition has the only significant contribution from HOMO-1–LUMO orbital transition. This reflects the single determinantal nature of the two transitions, and hence supports the use of time-dependent density functional theory (TD-DFT) for the calculations. The HOMO and LUMO orbital pictures in gas and different solvent phases are shown in Figure 2. The orbital pictures clearly indicate the short-range nature of the transitions. This is also supported by the larger values of Λ.

3.3. Two-Photon Absorption

After calculating the OPA parameters, we have calculated the TPA properties of the first two excited states of the concerned molecule. Firstly, we have calculated the TPA tensor elements (S_{ab})—which is related to the excitation energies and transition dipole moment vectors—by the following relation [37],

$$S_{ab} = \sum_n \left[\frac{\mu_a^{0n} \mu_b^{nf} + \mu_b^{0n} \mu_a^{nf}}{\Delta E_n} \right], \tag{2}$$

where $\Delta E_n = \omega_n - \frac{\omega_f}{2}$, and other terms have their usual meanings. The summation in Equation (2) runs over all the intermediate states, including the initial and final states. The TP transition probability for excitation by a linearly polarized single beam of light is related to S_{ab} through the following equation [38]:

$$\delta_{a.u.} = 6(S_{xx}^2 + S_{yy}^2 + S_{zz}^2) + 8(S_{xy}^2 + S_{xz}^2 + S_{yz}^2) + 4(S_{xx}S_{yy} + S_{xx}S_{zz} + S_{yy}S_{zz}) \tag{3}$$

The TPA cross-section is usually expressed in terms of Göppert Mayer (GM) unit. The relation between the GM and atomic unit is given by the following relation [39]:

$$\delta_{GM} = \frac{8\pi^2 \alpha a_0^5 \omega_f^2}{c\Gamma} \delta_{au}, \tag{4}$$

where α is the fine structure contstant, a_0 is the Bohr radius, c is the speed of light in vacuum, Γ is the line-shape function, and other terms have their usual meanings.

The results for S_{ab} and $\delta_{a.u.}$ are presented in Table 4. We noticed that, in solvent phases, the first excited state of D-luciferin is always much more TP active than the second excited state, whereas the reverse is true in gas phase. Furthermore, the TP activity of the first excited state in solvent phase is more than that in gas phase, whereas the TP activity of the second excited state in gas phase is more than that in solvent phase. In order to explain these results, we have performed a three-state model calculation based on the following generalized few-state model formula [21]:

$$\delta_{3SM} = \delta_{TP}^{11} + \delta_{TP}^{22} + 2\delta_{TP}^{12},$$
$$\delta_{TP}^{ij} = \frac{8\mu^{0i}\mu^{0j}\mu^{if}\mu^{jf}}{\Delta E_i \Delta E_i} \left(cos\theta_{0i}^{if} cos\theta_{0j}^{jf} + cos\theta_{0i}^{0j} cos\theta_{if}^{jf} + cos\theta_{0i}^{jf} cos\theta_{0j}^{if} \right), i, j = \{1, 2\} \tag{5}$$

where δ_{TP}^{ii} are the two-state terms, δ_{TP}^{ij} are the interference terms, and the angle θ_{ab}^{cd} represents the angle between the transition moment vectors μ^{ab} and μ^{cd}. The other terms in Equation (5) have their usual meanings. Within three-state model calculations, the ground state and the first two singlet excited states are included in Equation (5). The corresponding results are presented in Table 5. It is obvious from Table 5 that the 3SM results are in excellent qualitative as well as quantitative agreement with the quadratic response theory results. The role of channel interference is clearly visible for both the first and second excited states in D-luciferin. In both the gas and solvent phases, the channel interference

is always destructive in nature, which means it destroys the positive contribution from the $S_0 \rightarrow S_n$ transition in each case. This is because the pairwise angle terms (as appeared in Equation 5) are always negative. In both the gas and solvent phases, the contribution of channel interference for the second excited state is always larger in magnitude than that for the first excited state. In addition to this, the smaller μ^{02} values (as compared to μ^{01}) in solvent phases explains the lower TP activity of the second excited state, as compared to the first excited state. Note that the different behaviour of TP activity in gas phase (as revealed by the response theory) is also well reproduced by the three-state model (3SM). Both the response theory and 3SM indicates larger TP activity for the second excited state in gas phase, as compared to first excited state. 3SM indicates that the second excited state gains a significant amount of TP activity from the first excited state, as is obvious from larger δ^{11} value for the second excited state. 3SM also explains that, in polar solvent, the larger contribution of δ^{11} because of larger values of μ^{01} provides larger TP activity than that in non-polar or less-polar solvents.

Table 4. The two-photon absorption (TPA) tensor elements S_{ab} and TP transition probability for first and second excited states of D-luciferin molecule in gas and solvent phases.

Solvents	Excited States	S_{xx}	S_{yy}	S_{zz}	S_{xy}	S_{xz}	S_{yz}	$\delta_{a.u.}$ (10^4 a.u.)
Gas	1	96.3	2.1	0.9	27.1	1.6	−0.3	6.27
	2	−112.3	10.0	0.5	−1.0	−8.7	−4.1	7.23
C_2H_5OH	1	176.6	−2.8	0.7	31.4	7.1	1.9	19.41
	2	−74.2	12.1	1.0	13.7	−9.5	−4.6	3.24
$C_6H_5CH_3$	1	173.2	−1.8	0.8	33.8	6.4	1.6	18.87
	2	91.0	−13.0	−1.0	−11.3	10.1	4.9	4.77
C_6H_{12}	1	−166.0	1.5	−0.8	−33.1	−5.9	−1.4	17.40
	2	93.3	−12.7	−0.9	−10.1	9.9	4.8	4.98

Table 5. Three-state model results for TP transition probability, for the first two excited states of D-luciferin in gas and solvent phases. All the δ values are in 10^4 a.u., and angles are in degree.

Solvents	Excited States	δ_{TP}^{11}	δ_{TP}^{22}	$2\delta_{TP}^{12}$	δ_{3SM}	$\delta_{a.u.}$	θ_{01}^{1f}	θ_{02}^{2f}	θ_{01}^{02}	θ_{1f}^{2f}	θ_{01}^{2f}	θ_{02}^{1f}
Gas	1	0.95	5.26	−4.07	2.13	6.27	160.97	14.92	161.97	22.92	175.02	37.23
	2	11.80	1.05	−6.49	6.42	7.23	5.07	170.39	161.97	23.00	27.02	165.17
C_2H_5OH	1	24.30	0.11	−2.88	21.5	19.41	172.28	42.39	141.53	3.77	174.83	45.94
	2	3.92	1.16	−3.68	1.39	3.24	5.26	149.65	141.53	12.02	9.21	137.70
$C_6H_5CH_3$	1	21.0	0.49	−5.94	15.60	18.87	172.71	32.13	149.73	3.82	176.18	37.26
	2	8.24	2.01	−7.41	2.84	4.77	3.74	159.52	149.73	11.71	10.77	147.95
C_6H_{12}	1	18.3	0.66	−6.50	12.50	17.40	172.58	29.62	151.76	5.98	176.38	35.38
	2	9.12	2.14	−8.12	3.14	4.98	3.54	161.91	151.76	11.79	11.17	150.3

4. Conclusions

In this work, we present a theoretical study of one- and two-photon absorption properties for the first two singlet excited states of the D-luciferin molecule in gas and three different solvent (viz. ethanol, toluene, and cyclohexane) phases. For this purpose, we employ the linear and quadratic response theory within the framework of time-dependent density functional theory. Our results clearly indicate that—irrespective of the nature of medium (i.e., gas phase or solvent phase)—the first excited state of D-luciferin is always more one-photon active than its second excited state. We notice the larger value of transition dipole moment vector between ground and first excited state as the reason for this one-photon activity. We also notice that the x-component of the transition dipole moment is the most contributing component for the first excited state, whereas both the x and y components are contributing almost equally for the second excited state. This reflects that the $S_0 \rightarrow S_1$ transition is

mainly dominated by the charge-transfer from the donor to the acceptor group, whereas the $S_0 \rightarrow S_2$ transition has more contribution from the re-organization of the π electrons throughout the molecule. For two-photon excitation, the activity increases on moving from gas to solvent phases, and within solvents TP activity is maximum in polar solvents, which decreases in less polar or non-polar solvents. The first excited state is found to be more TP active than the second excited state. We explain these observations by analysing the corresponding three-state model calculations, which reflects the importance of channel interference on TP activity of both the two excited states. In the present case, the channel interference is always destructive in nature, because of the negative values of the pairwise angle terms appearing in the three-state model formula.

Author Contributions: Both the authors, Mausumi Chattopadhyaya and Md. Mehboob Alam were equally involved in the design of the project, computational work, data-analysis and writing of the manuscript.

Conflicts of Interest: The authors declare no conflict of interest.

References

1. Göppert-Mayer, M. Über elementarakte mit zwei quantensprüngen. *Ann. Phys.* **1931**, *9*, 237–294.
2. Barsu, B.; Cheaib, R.; Chambert, S.; Queneau, Y.; Maury, O.; Cottet, D.; Wege, H.; Douady, J.; Bretonniere, Y.; Andraud, C. Neutral push-pull chromophores for nonlinear optical imaging of cell membranes. *Org. Biomol. Chem.* **2010**, *8*, 142–150.
3. Lin, T.-C.; Huang, Y.-J.; Chen, Y.-F.; Hu, C.-L. Two-photon absorption and effective broadband optical power limiting properties of a multi-branched chromophore containing 2, 3-diarylquinoxalinyl moieties as the electron-pulling units. *Tetrahedron* **2010**, *66*, 1375–1382.
4. Hammerer, F.; Garcia, G.; Chen, S.; Poyer, F.; Achelle, S.; Fiorini-Debuisschert, C.; Teulade-Fichou, M.-P.; Maillard, P. Synthesis and characterization of glycoconjugated porphyrin triphenylamine hybrids for targeted two-photon photodynamic therapy. *J. Org. Chem.* **2014**, *79*, 1406–1417.
5. Kim, S.; Ohulchanskyy, Y.; Pudavar, H.E.; Pandey, R.K.; Prasad, P.N. Organically modified silica nanoparticles co-encapsulating photosensitizing drug and aggregation-enhanced two-photon absorbing fluorescent dye aggregates for two-photon photodynamic therapy. *J. Am. Chem. Soc.* **2007**, *129*, 2669–2675.
6. Pawlicki, M.; Collins, H.; Denning, R.; Anderson, H. Two-photon absorption and the design of two-photon dyes. *Angew. Chem. Int. Ed.* **2009**, *48*, 3244–3266.
7. Kawata, S.; Sun, H.B.; Tanaka, T.; Takada, K. Finer features for functional microdevices. *Nature* **2001**, *412*, 697.
8. Dvornikov, A.S.; Walker, E.P.; Rentzepis, P.M. Two-photon three-dimensional optical storage memory. *J. Phys. Chem. A* **2009**, *113*, 13633–13644.
9. Alam, M.M.; Chattopadhyaya, M.; Chakrabarti, S. On the origin of large two-photon activity of DANS molecule. *J. Phys. Chem. A* **2012**, *116*, 11034–11040.
10. Badaeva, E.A.; Timofeeva, T.V.; Masunov, A.; Tretiak, S. Role of donor-acceptor strengths and separation on the two-photon absorption response of cytotoxic dyes: A TD-DFT study. *J. Phys. Chem. A* **2005**, *109*, 7276–7284.
11. Yi, Y.; Li, Q.; Zhu, L.; Shuai, Z. Effects of donor/acceptor strengths on the multiphoton absorption: An EOM-CCSD correction vector study. *J. Phys. Chem. A* **2007**, *111*, 9291–9298.
12. Rubio-Pons, Ò.; Luo, Y.; Ågren, H. Very large infrared two-photon absorption cross section of asymmetric zinc porphyrin aggregates: Role of intermolecular interaction and donor-acceptor strengths. *J. Chem. Phys. A* **2006**, *110*, 12342–12347.
13. Wang, C.K.; Macak, P.; Luo, Y.; Ågren, H. Effects of π centers and symmetry on two-photon absorption cross sections of organic chromophores. *J. Chem. Phys.* **2001**, *114*, 9813–9820.

14. Chakrabarti, S.; Ruud, K. Large two-photon absorption cross section: Molecular tweezer as a new promising class of compounds for nonlinear optics. *Phys. Chem. Chem. Phys.* **2009**, *11*, 2592–2596.

15. Norman, P.; Luo, Y.; Ågren, H. Large two-photon absorption cross sections in two-dimensional, charge-transfer, cumulene-containing aromatic molecules. *J. Chem. Phys.* **1999**, *111*, 7758–7765.

16. Jha, P.C.; Rinkevicius, Z.; Ågren, H. Modeling two photon absorption cross sections of open-shell systems. *J. Chem. Phys.* **2009**, *130*, 014103.

17. He, G.S.; Tan, L.-S.; Zheng, Q.; Prasad, P.N. Multiphoton absorbing materials: molecular designs, characterizations, and applications. *Chem. Rev.* **2008**, *108*, 1245–1330.

18. Chattopadhyaya, M.; Alam, M.M.; Chakrabarti, S. New design strategy for the two-photon active material based on push–pull substituted bisanthene molecule. *J. Phys. Chem. A* **2011**, *115*, 2607–2614.

19. Cronstand, P.; Luo, P.; Ågren, H. Effects of dipole alignment and channel interference on two-photon absorption cross sections of two-dimensional charge-transfer systems. *J. Chem. Phys.* **2002**, *117*, 11102–11106.

20. Cronstand, P.; Luo, P.; Ågren, H. Generalized few-state models for two-photon absorption of conjugated molecules. *Chem. Phys. Lett.* **2002**, *352*, 262–269.

21. Alam, M.M.; Chattopadhyaya, M.; Chakrabarti, S. Solvent induced channel interference in the two-photon absorption process—A theoretical study with a generalized few-state-model in three dimensions. *Phys. Chem. Chem. Phys.* **2012**, *14*, 1156–1165.

22. Alam, M.M.; Chattopadhyaya, M.; Chakrabarti, S.; Ruud, K. Chemical control of channel interference in two-photon absorption processes. *Acc. Chem. Res.* **2014**, *47*, 1604–1612.

23. Luo, Y.; Norman, P.; Macak, P.; Ågren, H. Solvent-induced two-photon absorption of a push-pull molecule. *J. Phys. Chem. A* **2000**, *104*, 4718–4722.

24. Alam, M.M.; Kundi, V.; Thankachan, P.P. Solvent effects on static polarizability, static first hyperpolarizability and one-and two-photon absorption properties of functionalized triply twisted Möbius annulenes: A DFT study. *Phys. Chem. Chem. Phys.* **2016**, *18*, 21833–21842.

25. Ferrighi, L.; Frediani, L.; Fossgaard, E.; Ruud, K. Two-photon absorption of [2.2] paracyclophane derivatives in solution: A theoretical investigation. *J. Chem. Phys.* **2007**, *127*, 244103.

26. Alam, M.M.; Chattopadhyaya, M.; Chakrabarti, S.; Ruud, K. High-polarity solvents decreasing the two-photon transition probability of through-space charge-transfer systems–A surprising in silico observation. *J. Phys. Chem. Lett.* **2012**, *3*, 961–966.

27. Alam, M.M.; Chattopadhyaya, M.; Chakrabarti, S. A critical theoretical study on the two-photon absorption properties of some selective triaryl borane-1-naphthylphenyl amine based charge transfer molecules. *Phys. Chem. Chem. Phys.* **2011**, *13*, 9285–9292.

28. Alam, M.M. Donor's position-specific channel interference in substituted biphenyl molecules. *Phys. Chem. Chem. Phys.* **2015**, *17*, 17571–17576.

29. Miertus, S.; Scrocco, E.; Tomasi, J. Electrostatic interaction of a solute with a continuum. A direct utilizaion of AB initio molecular potentials for the prevision of solvent effects. *J. Chem. Phys.* **1981**, *55*, 117–129.

30. Tomasi, J.; Mennucci, B.; Cammi, R. Quantum mechanical continuum solvation models. *Chem. Rev.* **2005**, *105*, 2999–3094.

31. Frisch, M.J.; Trucks, G.W.; Schlegel, H.B.; Scuseria, G.E.; Robb, M.A.; Cheeseman, J.R.; Scalmani, G.; Barone, V.; Mennucci, B.; Petersson, G.A.; et al. *Gaussian-09*; Revision A.02; Gaussian Inc.: Wallingford, CT, USA, 2009.

32. Mikkelsen, K.V.; Ågren, H.; Jensen, H.J.A. A multiconfigurational self-consistent reaction-field method. *J. Chem. Phys.* **1988**, *89*, 3086–3095.

33. Mikkelsen, K.V.; Cesar, A.; Ågren, H.; Jensen, H.J.A. Multiconfigurational self-consistent reaction field theory for nonequilibrium solvation. *J. Chem. Phys.* **1995**, *103*, 9010–9023.

34. Aidas, K.; Angeli, C.; Bak, K.L.; Bakken, V.; Bast, R.; Boman, L.; Christiansen, O.; Cimiraglia, R.; Coriani, S.; Dahle, P.; et al. The Dalton quantum chemistry program system. *Wiley Interdiscip. Rev. Comput. Mol. Sci.* **2014**, *4*, 269–284.

35. Dalton, a Molecular Electronic Structure Program, Release Dalton, 2013.4, 2013. Available online: http://daltonprogram.org (accessed on 12 November 2016).

36. Conley, N.R.; Dragulescu-Andrasi, A.; Rao, J.; Moerner, W.E. A selenium analogue of firefly D-luciferin with red-shifted bioluminescence emission. *Angew. Chem. Int. Ed.* **2012**, *51*, 3350–3353.

37. Shen, Y.R. *The Principle of Nonlinear Optics*; Wiley: New York, NY, USA, 1984; pp. 23–25.

38. McClain, W.M. Excited state symmetry assignment through polarized wwo-photon absorption studies of fluids. *J. Chem. Phys.* **1971**, *55*, 2789–2796.

39. Murugan, N.A.; Kongsted, J.; Rinkevicius, Z.; Aidas, K.; Mikkelsen, K.V.; Ågren, H. Hybrid density functional theory/molecular mechanics calculations of two-photon absorption of dimethylamino nitro stilbene in solution. *Phys. Chem. Chem. Phys.* **2011**, *13*, 12506–12516.